Published in final edited form as:
Cancer Res. 2014 June 1; 74(11): 2986–2998. doi:10.1158/0008-5472.CAN-13-2689.

Fatty acid binding protein E-FABP restricts tumor growth by promoting IFNβ responses in tumor-associated macrophages

Yuwen Zhang[1], **Yanwen Sun**[1], **Enyu Rao**[1], **Fei Yan**[1], **Qiang Li**[1], **Ying Zhang**[2], **Kevin A. T. Silverstein**[2], **Shujun Liu**[1], **Edward Sauter**[3], **Margot P. Cleary**[1], and **Bing Li**[1,*]

[1]The Hormel Institute, University of Minnesota, Austin, MN 55912, USA

[2]Minnesota Supercomputing Institute, University of Minnesota, Minneapolis, MN, 55455, USA

[3]University of Texas Health Science Center, Tyler, TX, 75708, USA

Abstract

Fatty acid binding proteins (FABPs) are known central regulators of both metabolic and inflammatory pathways, but their role in tumor development remains largely unexplored. Here, we report that host expression of epidermal FABP (E-FABP) protects against mammary tumor growth. We find that E-FABP is highly expressed in macrophages, particularly in a specific subset, promoting their antitumor activity. In the tumor stroma E-FABP-expressing tumor-associated macrophages (TAMs) produce high levels of interferon β (IFNβ) through upregulation of lipid droplet (LD) formation in response to tumors. E-FABP-mediated IFNβ signaling can further enhance recruitment of tumoricidal effector cells, in particular NK cells, to the tumor stroma for antitumor activity. These findings identify E-FABP as a new protective factor to strengthen IFNβ responses against tumor growth.

Introduction

Fatty acid binding proteins (FABPs) constitute a family of intracellular lipid chaperones coordinating the distribution and function of lipids inside cells (1, 2). It has been well documented that FABPs play central roles in regulating metabolic and inflammatory pathways in various metabolic and autoimmune diseases (3–7). Given the dysregulated metabolic and inflammatory pathways during cancer development, FABPs have been suggested to participate in cancer initiation and progression. However, the exact mechanisms and functions of FABPs in these processes remain largely unknown. In our research focusing on epidermal FABP (E-FABP) functions, we have demonstrated that this protein is highly expressed in immune cells, especially in antigen presenting cells (APCs)

*To whom correspondence should be addressed: Bing Li, The Hormel Institute, University of Minnesota, 801 16th Avenue NE, Austin, MN 55912, USA. Telephone: 507-437-9623. Fax: 507-437-9606. bli@hi.umn.edu.

Disclosure of Potential Conflicts of Interest
The authors state no conflict of interest.

Authors' Contributions
Y.W.Z, Y.W.S., E.Y.R., F.Y., Q.L. performed research; Y.W.Z, Y.W.S. S.J.L, E.S and B.L. analyzed data; Y.Z., and K.S. carried out the microarray analysis; M.P.C. contributed to research design and manuscript writing. B.L. supervised the whole project, designed research and wrote the manuscript. All authors discussed the results and commented on the manuscript.

and T cells, and regulates both innate and adaptive immune responses (6, 8). Thus, we propose that E-FABP may link to tumor development through shaping host immune surveillance effects.

There is ample evidence indicating that interferons (IFNs) are critical in mediating immune surveillance to eradicate transformed cells through their effect on host hematopoietic cells (9, 10). Recent studies demonstrate that tumors can drive the production of IFNβ by host APCs to induce spontaneous adaptive T cell responses, further supporting the essential role of type I IFNs in antitumor immunity (11, 12). However, these seminal studies raise a number of important questions: 1) What is the specific population in the tumor stroma that can produce IFNβ in response to tumors? 2) How do the IFNβ-producing cells sense and interact with tumor cells? 3) Which molecule(s) or signaling pathway(s) is (are) critical in regulating IFNβ production? 4) How does IFNβ signaling lead to enhanced anti-tumor immunity? It is clear that tumor associated macrophages (TAMs) are the most abundant myeloid cells in tumors that exhibit phenotypic and functional heterogeneity (13–15). TAMs are classically divided into Th1 cytokine-induced M1 macrophages and Th2 cytokine-induced M2 macrophages. While M1 macrophages have been shown to produce abundant levels of pro-inflammatory cytokines, including type I IFNs, to perform antitumor activities (14, 16), it remains largely unknown which energetic provider is essential to support their anti-tumor functions.

Because there is high expression of E-FABP in macrophages and E-FABP, as a lipid chaperon, plays a critical role in regulating immune cell functions, we set out to assess whether host expression of E-FABP impacts tumor growth by shaping the function of the immune surveillance process in the present study. Specifically, we determined whether E-FABP displays a unique expression pattern in different subsets of macrophages and how E-FABP regulates specific macrophage antitumor function by focusing on IFNβ production and signaling.

Materials and Methods

Mice and human samples

E-FABP deficient (E-FABP$^{-/-}$) and wild type (WT) mice (C57BL/6 background) were bred and maintained in the animal facility of the Hormel Institute in accordance with approved protocols from the Institutional Animal Care and Use Committee (University of Minnesota). Mouse E0771 cells were from CH3 BioSystems; MC38 and RMA cells were gifts from Jun Yan (University of Louisville, KY). All cells were cultured less than 6 months for experiments. Cells were not further authenticated. Invasive breast cancer tissue microarray slides were purchased from US Biomax Inc (Rockville, MD). Human serum samples were collected from patients with benign breast diseases or invasive breast cancers. All patients provided informed consent under an IRB approved protocol.

Syngeneic mouse models

Different dosages of E0771 cells were orthotopically implanted into the mammary fat pad of 6–8 week old WT and E-FABP$^{-/-}$ mice. Tumors were measured at 3 day intervals with

calipers and the volume was calculated by the formula 0.4× (large diameter) × (small diameter)^2. E0771 cells were also intravenously injected into E-FABP$^{-/-}$ and WT mice to observe tumor metastasis in lungs. For NK cell- or CD4$^+$ T cell-depletion assay, mice were intraperitoneally injected with anti-NK1.1 or anti-CD4 neutralizing mAb, respectively. After confirmation of the depletion of NK cells or CD4$^+$ T cells, mice were implanted with E0771 cells as described above. To measure immune cell infiltration and functions in tumor stroma, single cells from solid tumors were prepared by digesting dissected tumors in an enzyme mixture (0.5 mg/ml collagenase A, 0.2 mg/ml type V hyaluronidase and 0.02 mg/ml DNase I in RPMI 1640) at 37°C for 45 min. The separated cells were washed for further analyses.

Flow Cytometric analysis and cell sorting

Surface and intracellular staining were performed as previously described (8). Single immune cell populations in spleens or tumors were separated with a BD FACSAria II Cell Sorter. Flow cytometric analyses were performed with Flowjo (Tree Star). The detailed antibody clone information is shown in the supplemental materials and methods.

Gene Expression Microarray

1×10^6 GM-CSF-induced bone marrow-derived macrophages (GM-BMMs) from WT and E-FABP$^{-/-}$ mice were cocultured with 2×10^6 E0771 cells in a transwell plate for 24h. Total RNA was extracted from tumor-stimulated GM-BMMs using RNeasy Mini Kit (Qiagen) and subjected to mouse mRNA Gene expression by Affymetrix microarray. Microarray analysis was performed using R/Bioconductor packages and signaling pathway was generated with Ingenuity Pathways Analysis (IPA) (Ingenuity Systems). The expression profiling data were submitted to the Gene Expression Omnibus (GSE54073).

Quantitative real-time PCR

RNA was extracted from cultured or purified primary cells using RNeasy Mini Kit (Qiagen). cDNA synthesis was performed with QuantiTect Reverse Transcription Kit (Qiagen). Quantitative PCR was performed with SYBR® Green PCR Master Mix using ABI 7500 Real-Time PCR Systems (Applied Biosystems). Detailed primer sequences are shown in the supplemental information.

Western Blotting

To quantify the protein levels of E-FABP, A-FABP, phosphorylation and total STAT1 and STAT2, macrophages with designated treatments were lysed in buffers with protease and phosphorylation inhibitors. Protein concentration was determined by BCA assay (Thermo Scientific). β-actin was used as a loading control. Mouse E-FABP, A-FABP, β-actin antibodies were from R&D Systems. Mouse STAT1, STAT2 and their phosphorylation antibodies were from Cell Signaling Technology.

Confocal Analysis

GM-BMMs cultured on poly-D-lysine coated coverslips (NeuVitro) in a 24-well plate were treated with saturated FAs (stearic acid) or unsaturated FAs (oleic/linoleic acid) for 24 hours. After fixation and permeabilization, the cells were stained with BODIPY® 493/503

(Invitrogen) and/or Viperin (Millipore). Nuclei were stained with 0.2μM DAPI (Invitrogen). For lipid droplet inhibition assay, GM-BMMs were treated with designated Triacsin C plus unsaturated FAs for 24h before analysis. For measurement of E-FABP expression, macrophages or breast cancer tissue microarray slides were stained with E-FABP specific antibody (R&D System). Confocal analysis was performed with Nikon Eclipse TE2000 confocal microscopy.

ELISA

GM-BMMs (0.5×10^6) from WT and E-FABP$^{-/-}$ mice were cocultured with 1×10^6 E0771 tumor lysates (obtained after freezing in liquid nitrogen and thawing at 37°C for 3~4 cycles) for 3 hours. The supernatants were collected for measurement of IFNβ with ELISA kit (Biolegend). For analysis of IFNβ production in E-FABP knockdown macrophages, macrophages were transfected with On-target plus E-FABP siRNA or scramble oligos (Thermo Dharmacon) using Lipofectamine™ RNAiMAX (Life Technologies) and stimulated with LPS (100ng/ml) before supernatant collection.

Tumor Killing Assays

Lymphocytes collected from draining lymph nodes of E0771-tumor bearing mice were used as effector cells. Target cells (E0771) were labeled with 2μM CFSE. Effector and target cells were cocultured for 22 hours in a 96-well v-bottom plate in the presence or absence of blocking antibodies to TRAIL, CD4, CD8 and NK cells, respectively. All cells were stained with 7-AAD and analyzed by flow cytometry. Tumor specific killing was calculated as the difference between total % of killed (7-AAD$^+$) and % of spontaneous apoptotic E0771 cells in all CFSE$^+$ tumor cells.

Statistical Analysis

For analysis of microarray data, Affy and Limma packages were used to perform the data prepping steps and implement linear models for differential expression. A false discovery rate (FDR) corrected P value was used to filter out the differentially expressed probes. Unpaired, two-tailed Student's *t* test was performed for the comparison of results from other different treatments. $P<0.05$ is considered statistically significant.

Results

Host expression of E-FABP suppresses tumor growth

To determine the contribution of host expression of E-FABP to tumor growth, E0771 tumor cells, originally from a C57BL/6 mouse mammary adenocarcinoma (17), were orthotopically injected into the mammary fat pad of E-FABP$^{-/-}$ mice and their WT littermates. Tumor growth was measured in a 3-week period after tumor implantation (Fig. 1A). Mammary tumors in E-FABP$^{-/-}$ mice grew 3-fold faster as compared to those in WT mice (Fig.1B). Final tumor weights in E-FABP$^{-/-}$ mice were also 3-fold heavier than tumors that formed in WT mice (Fig.1C). Furthermore, E-FABP deficiency markedly increased E0771 tumor lung metastasis as demonstrated by metastatic spots ($p=0.011$) (Fig.1D) and tumor size (Fig.1E). Experiments with tail vein injection of E0771 cells also demonstrated increased lung tumor burden in the absence of E-FABP (Fig.1F,1G). Of note, when we

titrated the dosage of injected tumor cells in mice, we found that the more E0771 cells we injected, the less pronounced was the difference in tumor growth between WT and E-FABP −/− mice (Supplementary Fig.1A), suggesting that host expression of E-FABP does not provide unlimited protection to tumor challenges. To further confirm the protective role of E-FABP, we evaluated tumor burden with other C57BL/6-derived murine tumor cells, i.e., the lymphoma cell line, RMA, and the colon cancer cell line, MC38, in E-FABP$^{-/-}$ and WT mice. Similar to E0771 cells, these additional cell lines exhibited increased tumor burden when E-FABP was absent in mice (Supplementary Fig.1B,1C). These results clearly show that host expression of E-FABP is critical in suppressing tumor growth.

E-FABP is highly expressed in macrophages

To understand how E-FABP contributes to tumor protection, we first examined the expression profile of E-FABP in naïve mice. F4/80^{+} macrophages expressed the highest levels of E-FABP among splenic leukocyte subsets, 9 fold higher than adipocytes (Fig.2A). Immunostaining of mammary fat tissue (Fig.2B) and purified populations from peripheral blood (Fig.2C) showed that E-FABP was also highly expressed in F4/80^{+} cells. Using bone marrow-derived macrophages, we further confirmed that E-FABP was specifically located in the cytoplasm of WT macrophages, but not in the E-FABP$^{-/-}$ cells (Fig.2D,2E). Next, we compared immune cell phenotypes of naïve and E0771 tumor-bearing mice with a focus on TAMs. Compared to spleens and draining lymph nodes (dLNs) in naïve mice, tumor-bearing mice exhibited both enlarged spleens and dLNs with significantly higher numbers of total cells (Supplementary Fig.2A,2B). Further analysis showed the enlarged spleens and dLNs were associated with increased CD11b^{+}F4/80^{+} macrophages, but not with CD4^{+}, CD8^{+} NK1.1^{+}, and CD11c^{+} populations (Fig.2F,2G). Consistently, we found a large quantity of myeloid-derived macrophages (CD11b^{+}F4/80^{+}) infiltrated in tumors from WT and E-FABP$^{-/-}$ mice (Fig.2H,2I and Supplementary Fig.2C). As TAMs play critical roles during cancer development (13, 18–20), these results suggest that E-FABP expression in macrophages may protect against tumor growth by promoting their antitumor mechanisms.

Identification of E-FABP expression in specific subsets of macrophages

It is well known that TAMs consist of distinct subpopulations with specialized functions in tumors (21–23). We speculated that E-FABP might exhibit unique expression patterns in different subsets of TAMs. First, we used anti-Ly6C and anti-MHCII antibodies to identify distinct subsets of splenic macrophages (CD11b^{+}F4/80^{+}) from naïve mice (Fig.3A,3B), and found that each subset exhibited different levels of CD11c expression (Fig.3C,3D). Importantly, we demonstrated for the first time that E-FABP was highly expressed in the Q2 and Q3 subsets which exhibited the F4/80^{+}CD11b^{+}MHCII^{+}CD11c^{+} phenotype. In contrast, Q1 and Q4 subsets exhibited no or very low levels of E-FABP expression (Fig.3E). To further examine the E-FABP expression pattern in TAMs, we collected E0771 tumors from WT and E-FABP$^{-/-}$ mice at different time points. Strikingly, TAM subsets exhibited dynamic changes during tumor development (Fig.3F). Among the distinct subsets, we found that the Q2 subset, peaking on day 7 after tumor implantation (Supplementary Fig.3A), expressed the highest levels of CD11c (Fig.3G) and E-FABP (Fig.3H). Although the Q2 subset declined progressively thereafter, E-FABP expression in this subset remained at higher levels relative to the same subset in the spleen during tumor development

(Supplementary Fig.3B). As the MHCII^{+}CD11c^{+} macrophages display a more M1-like phenotype while the MHCII^{-}CD11c^{-} subset is more M2-oriented in tumors (14, 23), our data demonstrate a unique expression pattern of E-FABP in M1-like macrophages, suggesting distinct functions of this subset through expression of E-FABP.

Promotion of IFNβ responses in macrophages by E-FABP

As GM-BMMs expressed high levels of CD11b, F4/80, MHCII, CD11c, and E-FABP expression (Supplementary Fig.4A–4D), exhibiting a similar phenotype to E-FABP-expressing TAMs as described above, we thus used GM-BMMs from WT and E-FABP−/− mice to dissect how E-FABP expression in specific TAMs contributes to their antitumor activity. We first performed Affymetrix microarray experiments to analyze the E0771 tumor-stimulated gene expression profiles with these cells. The selected differentially expressed genes with $p<0.05$ between WT and E-FABP$^{-/-}$ macrophages are shown in the Supplementary Table 1. A heat map of 33 most differentially expressed genes in response to E0771 stimulation between WT and E-FABP$^{-/-}$ GM-BMMs is shown in Figure 4A. Very intriguingly, IPA pathway analysis suggested that E-FABP expression in macrophages primarily regulates inflammatory responses, especially IFNβ responses (Supplementary Fig. 4E). We further confirmed the microarray results with real-time PCR. E-FABP-expressing macrophages exhibited significant upregulation of IFNβ response-related genes, such as Viperin, IRF-7, IFNβ, CXCL10, CXCL11, Lipg1, and other M1-related molecules, such as TNFSF10 (24), Ms4a4c (25), as compared to E-FABP$^{-/-}$ macrophages (Fig.4B and Supplementary Fig.4F). Moreover, the levels of secreted IFNβ in supernatants of E-FABP$^{-/-}$ macrophages were significantly lower than that in WT macrophages with stimulation of tumor lysates (Fig.4C). Knockdown of E-FABP with E-FABP siRNA also inhibited IFNβ production in macrophages (Fig.4D,4E). Altogether, these results indicate that E-FABP is essential to promote IFNβ responses in macrophages.

E-FABP regulates IFNβ responses through controlling lipid droplet formation

Since lipid droplets (LDs) function as platforms to bind Viperin which controls type I IFN induction (26, 27), we speculate that E-FABP as a lipid transporter may control LD formation to regulate IFNβ responses. As GM-BMMs predominantly expressed E-FABP (Supplementary Fig.5A,5B), we used these cells to dissect the effect of E-FABP-mediated LDs for IFNβ production. Compared to saturated stearic acid, unsaturated oleic/linoleic acids were more effective in enhancing E-FABP expression and LD formation in WT GM-BMMs. More importantly, FA-enhanced LD formation was markedly decreased in the absence of E-FABP in macrophages (Fig.5A,5B). In line with this observation, the production of Viperin and IFNβ was significantly decreased in E-FABP$^{-/-}$ macrophages as compared to WT macrophages (Fig.5C,5D). To determine the essential role of LDs for IFNβ production, we inhibited LD formation in macrophages with Triacsin C(28), a potent LD inhibitor (Supplementary Fig.5C), and confirmed that LD inhibition indeed impaired IFNβ production in macrophages (Fig.5E). As oleic acid and linoleic acid are the two most common unsaturated FAs derived from tumor membranes (29), we cocultured macrophages with E0771 tumor cells and demonstrated that E-FABP enhanced LD formation and Viperin production in tumor-stimulated macrophages (Fig.5F,5G). To measure whether E-FABP regulates IFNβ signaling, we found that E-FABP$^{-/-}$ macrophages exhibited reduced

phosphorylation of STAT1 and STAT2 as compared to WT cells in response to IFNβ stimulation (Fig. 5H,5I). Consistently, when the Q2 subset of TAMs was separated from early stage E0771 tumors, TAMs from WT mice exhibited markedly enhanced levels of E-FABP, Viperin, IRF7, IFNβ, CXCL10 and CXCL11 as compared to the same population from E-FABP$^{-/-}$ mice (Fig.5J–5O), further verifying the attenuated IFNβ responses by E-FABP deficiency in TAMs. Thus, E-FABP can regulate IFNβ responses through controlling LD formation in specific TAMs.

IFNβ signaling enhances recruitment of tumoricidal effector cells

It has been clear that inflammatory chemokines, such as CXCL10 and CXCL11, can recruit effector T cells and NK cells to inflamed tissues (30, 31), which produce a large amount of IFNγ for immune surveillance. As IFNβ-producing TAMs highly expressed CXCL10 and CXCL11 in WT mice, we speculated that more effector T cells and NK cells accumulated in these mice to promote their antitumor activity. Indeed, we observed a significantly higher percentage of CD4$^+$ T cells, CD8$^+$ T cells and NK cells in tumors from WT mice than in tumors from E-FABP$^{-/-}$ mice in the first week post tumor implantation (Fig.6A–6C). Notably, the difference disappeared in the late stage of tumor growth (3 weeks post E0771 cell implantation, Fig. 2I), implying an early effect of E-FABP protection. In addition, E-FABP deficiency had no significant impact on IFNγ production from these infiltrating cells (Supplementary Fig.6A–6C). To determine whether these effector cells were responsible for tumor cytotoxicity, we cocultured them with CSFE-labeled tumor cells and demonstrated that effector cells from WT dLNs exhibited higher tumor killing activity than these from E-FABP$^{-/-}$ dLNs (Fig. 6D). Assays with blocking antibodies specific to CD4, CD8, NK or TRAIL (TNFSF10) suggested that NK cells were the main effector cells in mediating tumor killing *in vitro* (Fig. 6E). To confirm this observation, we depleted NK cells in WT and E-FABP$^{-/-}$ mice (Fig. 6F and Supplementary Fig.6D) and demonstrated that the tumor-suppressive effect of E-FABP in WT mice diminished in the absence of NK cells (Fig. 6G). In contrast, depletion of CD4$^+$ T cells did not affect tumor growth in both WT and E-FABP$^{-/-}$ mice (Supplementary Fig.7). Thus, E-FABP-regulated IFNβ signaling in specific TAMs can recruit effector cells, particularly NK cells, for tumor killing.

E-FABP expression in TAMs in human breast cancers

Due to the tumor protective role of E-FABP in mouse models, we next examined whether E-FABP was downregulated in human breast cancers. We analyzed E-FABP expression in normal and malignant breast tissues using publicly accessible microarray data. We found that E-FABP was significantly decreased in various types of breast cancers, including invasive ductal carcinoma, invasive lobular carcinoma and mucinous carcinoma, as compared to normal tissues (Fig.7A). Interestingly, the statistical significance positively correlated with the sample size (Supplementary Table 2), suggesting a real effect of E-FABP reduction in breast cancers. By analyzing E-FABP expression in breast stroma tissues with a GEO dataset GSE9014 (20), we found that E-FABP was markedly down-regulated in stroma of invasive human breast tumors as compared to normal stroma (Fig.7B and Supplementary Table 3), further corroborating the importance of E-FABP expression in tumor stroma for breast cancer protection. To dissect the location of E-FABP expression in tumor stroma, we used confocal microscopy staining to analyze the expression pattern of E-FABP and TAMs

in a tissue microarray containing samples from women with different stages of disease. We found E-FABP was highly expressed in TAMs of women with early stage disease, decreasing with disease progression (Fig.7C,7D), which was similar to what we observed in mouse models. In addition, we measured circulating levels of E-FABP in patients with benign breast diseases or breast cancer patients and found no differences between them (Supplementary Fig.8A,8B). Addition of soluble E-FABP directly to the culture media impacted neither the migration of breast cancer MDA-MB-231 cells nor their colony formation (Supplementary Fig.8C, 8D). These results suggest that circulating E-FABP is not associated with breast cancer development. Altogether, our findings support the idea that E-FABP exerts its protective role through regulation of TAM functions.

Discussion

Compelling evidence from mouse and human studies indicates the importance of immune surveillance of tumors. Thus, how to strengthen host immunity to protect against tumor development remains an area of intense research (32, 33). It is clear that optimal immune surveillance function depends on appropriate energetic support and homeostasis (34). We and others have observed that E-FABP is expressed highly in macrophages, less in adipocytes and is barely detectable in non-invasive breast cell lines (35), indicating that E-FABP plays an important role in regulating macrophage functions. While recent studies suggest that E-FABP ectopic expression in tumor cells can promote their invasive phenotype (36, 37), our data clearly demonstrate that E-FABP as a cytoplasmic energy carrier enhances the effects of macrophage immune surveillance by promoting LD formation and IFNβ responses in response to tumors. Thus, E-FABP expression in macrophages represents a new mechanism to protect against tumor growth.

To dissect how E-FABP enhances macrophage antitumor activity, we investigated E-FABP expression in different subsets of macrophages and identified that E-FABP is highly expressed in a specific subset which exhibits the $CD11b^{+}F4/80^{+}Ly6c^{+}CD11c^{+}MHCII^{+}$ phenotype (Fig.3). More intriguingly, this subset reached peak levels in the tumor stroma in the first week post tumor implantation and declined thereafter, implying that E-FABP-mediated protection is initiated in the early stage of tumor development. While not influencing TAM infiltration, E-FABP expression in specific TAMs promotes their production of IFNβ. Consistent with previous studies identifying $CD11c^{+}$ APCs as the source of IFNβ production in tumors (12, 38), our data further define the phenotype of these IFNβ-producing cells and identify the importance of E-FABP in mediating IFNβ responses in this specific subset.

The continuous death of malignant cells during the tumorigenic process results in uptake of macrophages as well as a range of immune responses within the tumor (39). While much attention has been focused on tumor-released proteins and nucleic acids in triggering host immune responses (40, 41), it is largely unknown how macrophages deal with the large pieces of lipid debris produced from dying tumor cells. In exploring E-FABP as a new sensing factor mediating macrophage-tumor interactions, our data suggest that specific macrophages can employ tumor-derived lipids through upregulation of E-FABP to support their antitumor function. Mechanistically, E-FABP-mediated lipid transportation enhances

energy storage and LD formation in macrophages. LDs not only provide lipids for energy metabolism, but also regulate intracellular immune responses through binding specific signaling proteins (42). It has been shown that Viperin, an IFN-stimulated protein, is anchored with its N-terminus α-helix domain to LDs to mediate IFNβ production (43, 44). Our data provide experimental evidence that macrophage-tumor interaction promotes E-FABP-mediated LD formation and increases Viperin and IFNβ production in macrophages. In contrast, inhibition of LD formation significantly impairs IFNβ production (Fig.5). Thus, LDs play an essential role for IFNβ production in macrophages, which contributes to our increasing understanding of lipid droplet functions (45).

IFN responses usually consist of two phases: 1) the production of IFNs by innate cells in response to infection, autoimmunity or tumor stimulation, and 2) the binding of secreted IFNs to IFN receptor to activate JAK-STAT signaling and induce IFN-stimulated genes (ISGs) (26). Our data demonstrate that E-FABP affects not only the production of IFNβ in response to tumors, but also the phosphorylation of STAT1 and STAT2, and the expression of ISGs, such as CXCL10, CXCL11, CCL12, LIPG1 and TNFSF10 (Fig.4,5). Of note, E-FABP deficiency has no impact on the expression of IFNβ receptor expression (Supplementary Fig.4F). To explore how E-FABP-regulated IFNβ responses enhance host antitumor immunity, we found that increased numbers of effector cells, including T cells and NK cells, are recruited into the tumor milieu of WT mice. We further identified that NK cells are the major effector cells in mediating tumor immunosurveillance effect of E-FABP (Fig.6), which is consistent with previous studies showing that NK cells are the main IFN targets for antitumor responses (46, 47). Although E-FABP has been shown to promote Th17-cell differentiation in the model of experimental autoimmune encephalomyelitis (8), we did not observe any significant IL-17-producing $CD4^+$ T cells in tumor stroma of the tested tumor models (data not shown). Instead, IFNγ is largely produced by infiltrated T cells and NK cells, but E-FABP deficiency does not significantly affect IFNγ production (Supplementary Fig.6). Thus, E-FABP promotes IFNβ production and signaling in specific macrophages, which further increases the recruitment of effector cells, especially NK cells, for tumor killing, thereby leading to reduced tumor growth. As E-FABP deficiency has no impact on the production of prometastatic molecules (e.g. MMPs, VEGF) in macrophages as indicated from our microarray analyses, it is possible that, compared to E-$FABP^{-/-}$ mice, the reduced tumor lung metastasis in E-FBBP sufficient mice is due to the increased tumor killing in these mice.

Since E-FABP expression strengthens host antitumor immune surveillance, it is logical to speculate that established tumors may exhibit decreased expression of E-FABP. Indeed, E-FABP levels in different types of human breast cancer tissues are significantly lower as compared to normal breast tissues. As our mouse studies indicate that E-FABP is highly expressed in macrophages in tumor stroma, further analysis with human breast stroma tissues demonstrated that E-FABP expression is markedly reduced in the stroma of invasive breast cancers. In addition, we confirmed that E-FABP is mainly expressed in TAMs in human breast cancer tissues and the numbers of E-FABP expressing TAMs are significantly reduced in advanced stages of invasive breast cancers (Fig.7). While macrophages are generally considered to contribute to tumor progression through enhancing angiogenesis,

migration and invasion (15, 48), our research points out that a specific subset of TAMs, which highly express E-FABP, perform strong antitumor activity.

In summary, we find that E-FABP is highly expressed in a specific subset of macrophages, which produce large amounts of IFNβ triggered by tumors. Mechanistically, E-FABP promotes IFNβ responses through the control of LD formation during macrophage-tumor interactions, which further enhance recruitment of tumoricidal effector cells for tumor killing. Thus, E-FABP represents a new protective factor in the control of cancer.

Supplementary Material

Refer to Web version on PubMed Central for supplementary material.

Acknowledgments

The authors thank Dr. Jill Suttles for providing us E-FABP deficient mice and the Mayo Clinic Gene Expression Core for the help of performing Affymetrix microarray.

Grant Support

This work was supported by the Hormel Foundation (B. Li), Hormel Institute Breast Cancer Research Grant (PTTP, B. Li), Minnesota Obesity Center (Pilot & Feasibility project, B. Li), Career Transition Fellowship (NMSS, TA3047-A-1, B. Li), and NIH R01-CA157012 (M.P.C)

Reference List

1. Furuhashi M, Hotamisligil GS. Fatty acid-binding proteins: role in metabolic diseases and potential as drug targets. Nat Rev Drug Discov. 2008; 7:489–503. [PubMed: 18511927]
2. Hertzel AV, Bernlohr DA. The mammalian fatty acid-binding protein multigene family: molecular and genetic insights into function. Trends Endocrinol Metab. 2000; 11:175–180. [PubMed: 10856918]
3. Furuhashi M, Tuncman G, Gorgun CZ, Makowski L, Atsumi G, Vaillancourt E, et al. Treatment of diabetes and atherosclerosis by inhibiting fatty-acid-binding protein aP2. Nature. 2007; 447:959–965. [PubMed: 17554340]
4. Maeda K, Cao H, Kono K, Gorgun CZ, Furuhashi M, Uysal KT, et al. Adipocyte/macrophage fatty acid binding proteins control integrated metabolic responses in obesity and diabetes. Cell Metab. 2005; 1:107–119. [PubMed: 16054052]
5. Milner KL, van der Poorten D, Xu A, Bugianesi E, Kench JG, Lam KS, et al. Adipocyte fatty acid binding protein levels relate to inflammation and fibrosis in nonalcoholic fatty liver disease. Hepatology. 2009; 49:1926–1934. [PubMed: 19475694]
6. Reynolds JM, Liu Q, Brittingham KC, Liu Y, Gruenthal M, Gorgun CZ, et al. Deficiency of fatty acid-binding proteins in mice confers protection from development of experimental autoimmune encephalomyelitis. J Immunol. 2007; 179:313–321. [PubMed: 17579051]
7. Xu A, Tso AW, Cheung BM, Wang Y, Wat NM, Fong CH, et al. Circulating adipocyte-fatty acid binding protein levels predict the development of the metabolic syndrome: a 5-year prospective study. Circulation. 2007; 115:1537–1543. [PubMed: 17389279]
8. Li B, Reynolds JM, Stout RD, Bernlohr DA, Suttles J. Regulation of Th17 differentiation by epidermal fatty acid-binding protein. J Immunol. 2009; 182:7625–7633. [PubMed: 19494286]
9. Dunn GP, Bruce AT, Sheehan KC, Shankaran V, Uppaluri R, Bui JD, et al. A critical function for type I interferons in cancer immunoediting. Nat Immunol. 2005; 6:722–729. [PubMed: 15951814]
10. Smyth MJ. Type I interferon and cancer immunoediting. Nat Immunol. 2005; 6:646–648. [PubMed: 15970935]

11. Fuertes MB, Kacha AK, Kline J, Woo SR, Kranz DM, Murphy KM, et al. Host type I IFN signals are required for antitumor CD8+ T cell responses through CD8{alpha}+ dendritic cells. J Exp Med. 2011; 208:2005–2016. [PubMed: 21930765]
12. Fuertes MB, Woo SR, Burnett B, Fu YX, Gajewski TF. Type I interferon response and innate immune sensing of cancer. Trends Immunol. 2012
13. Condeelis J, Pollard JW. Macrophages: obligate partners for tumor cell migration, invasion, and metastasis. Cell. 2006; 124:263–266. [PubMed: 16439202]
14. Mantovani A, Sica A. Macrophages, innate immunity and cancer: balance, tolerance, and diversity. Curr Opin Immunol. 2010; 22:231–237. [PubMed: 20144856]
15. Pollard JW. Tumour-educated macrophages promote tumour progression and metastasis. Nat Rev Cancer. 2004; 4:71–78. [PubMed: 14708027]
16. Mosser DM, Edwards JP. Exploring the full spectrum of macrophage activation. Nat Rev Immunol. 2008; 8:958–969. [PubMed: 19029990]
17. Ewens A, Mihich E, Ehrke MJ. Distant metastasis from subcutaneously grown E0771 medullary breast adenocarcinoma. Anticancer Res. 2005; 25:3905–3915. [PubMed: 16312045]
18. Mantovani A, Marchesi F, Porta C, Sica A, Allavena P. Inflammation and cancer: breast cancer as a prototype. Breast. 2007; 16(Suppl 2):S27–S33. [PubMed: 17764938]
19. Beck AH, Espinosa I, Edris B, Li R, Montgomery K, Zhu S, et al. The macrophage colony-stimulating factor 1 response signature in breast carcinoma. Clin Cancer Res. 2009; 15:778–787. [PubMed: 19188147]
20. Finak G, Bertos N, Pepin F, Sadekova S, Souleimanova M, Zhao H, et al. Stromal gene expression predicts clinical outcome in breast cancer. Nat Med. 2008; 14:518–527. [PubMed: 18438415]
21. Laoui D, Movahedi K, Van OE, Van den Bossche J, Schouppe E, Mommer C, et al. Tumor-associated macrophages in breast cancer: distinct subsets, distinct functions. Int J Dev Biol. 2011; 55:861–867. [PubMed: 22161841]
22. Lewis CE, Pollard JW. Distinct role of macrophages in different tumor microenvironments. Cancer Res. 2006; 66:605–612. [PubMed: 16423985]
23. Movahedi K, Laoui D, Gysemans C, Baeten M, Stange G, Van den Bossche J, et al. Different tumor microenvironments contain functionally distinct subsets of macrophages derived from Ly6C(high) monocytes. Cancer Res. 2010; 70:5728–5739. [PubMed: 20570887]
24. Hallam S, Escorcio-Correia M, Soper R, Schultheiss A, Hagemann T. Activated macrophages in the tumour microenvironment-dancing to the tune of TLR and NF-kappaB. J Pathol. 2009; 219:143–152. [PubMed: 19662665]
25. Murray RZ, Wylie FG, Khromykh T, Hume DA, Stow JL. Syntaxin 6 and Vti1b form a novel SNARE complex, which is up-regulated in activated macrophages to facilitate exocytosis of tumor necrosis Factor-alpha. J Biol Chem. 2005; 280:10478–10483. [PubMed: 15640147]
26. Jiang X, Chen ZJ. Viperin links lipid bodies to immune defense. Immunity. 2011; 34:285–287. [PubMed: 21435581]
27. Saitoh T, Satoh T, Yamamoto N, Uematsu S, Takeuchi O, Kawai T, et al. Antiviral protein Viperin promotes Toll-like receptor 7- and Toll-like receptor 9-mediated type I interferon production in plasmacytoid dendritic cells. Immunity. 2011; 34:352–363. [PubMed: 21435586]
28. Namatame I, Tomoda H, Arai H, Inoue K, Omura S. Complete inhibition of mouse macrophage-derived foam cell formation by triacsin C. J Biochem. 1999; 125:319–327. [PubMed: 9990129]
29. Kobayashi N, Barnard RJ, Henning SM, Elashoff D, Reddy ST, Cohen P, et al. Effect of altering dietary omega-6/omega-3 fatty acid ratios on prostate cancer membrane composition, cyclooxygenase-2, and prostaglandin E2. Clin Cancer Res. 2006; 12:4662–4670. [PubMed: 16899616]
30. Kurachi M, Kurachi J, Suenaga F, Tsukui T, Abe J, Ueha S, et al. Chemokine receptor CXCR3 facilitates CD8(+)T cell differentiation into short-lived effector cells leading to memory degeneration. J Exp Med. 2011; 208:1605–1620. [PubMed: 21788406]
31. Wendel M, Galani IE, Suri-Payer E, Cerwenka A. Natural killer cell accumulation in tumors is dependent on IFN-gamma and CXCR3 ligands. Cancer Res. 2008; 68:8437–8445. [PubMed: 18922917]

32. Dunn GP, Koebel CM, Schreiber RD. Interferons, immunity and cancer immunoediting. Nat Rev Immunol. 2006; 6:836–848. [PubMed: 17063185]
33. Swann JB, Smyth MJ. Immune surveillance of tumors. J Clin Invest. 2007; 117:1137–1146. [PubMed: 17476343]
34. Wellen KE, Hotamisligil GS. Inflammation, stress, and diabetes. J Clin Invest. 2005; 115:1111–1119. [PubMed: 15864338]
35. Kannan-Thulasiraman P, Seachrist DD, Mahabeleshwar GH, Jain MK, Noy N. Fatty acid-binding protein 5 and PPARbeta/delta are critical mediators of epidermal growth factor receptor-induced carcinoma cell growth. J Biol Chem. 2010; 285:19106–19115. [PubMed: 20424164]
36. Levi L, Lobo G, Doud MK, von LJ, Seachrist D, Tochtrop GP, et al. Genetic ablation of the fatty acid binding protein FABP5 suppresses HER2-induced mammary tumorigenesis. Cancer Res. 2013
37. Liu RZ, Graham K, Glubrecht DD, Germain DR, Mackey JR, Godbout R. Association of FABP5 expression with poor survival in triple-negative breast cancer: implication for retinoic acid therapy. Am J Pathol. 2011; 178:997–1008. [PubMed: 21356353]
38. Diamond MS, Kinder M, Matsushita H, Mashayekhi M, Dunn GP, Archambault JM, et al. Type I interferon is selectively required by dendritic cells for immune rejection of tumors. J Exp Med. 2011; 208:1989–2003. [PubMed: 21930769]
39. Fonseca C, Dranoff G. Capitalizing on the immunogenicity of dying tumor cells. Clin Cancer Res. 2008; 14:1603–1608. [PubMed: 18347160]
40. Tesniere A, Apetoh L, Ghiringhelli F, Joza N, Panaretakis T, Kepp O, et al. Immunogenic cancer cell death: a key-lock paradigm. Curr Opin Immunol. 2008; 20:504–511. [PubMed: 18573340]
41. Wang Z, Choi MK, Ban T, Yanai H, Negishi H, Lu Y, et al. Regulation of innate immune responses by DAI (DLM-1/ZBP1) and other DNA-sensing molecules. Proc Natl Acad Sci U S A. 2008; 105:5477–5482. [PubMed: 18375758]
42. Walther TC, Farese RV Jr. Lipid droplets and cellular lipid metabolism. Annu Rev Biochem. 2012; 81:687–714. [PubMed: 22524315]
43. Hinson ER, Cresswell P. The N-terminal amphipathic alpha-helix of viperin mediates localization to the cytosolic face of the endoplasmic reticulum and inhibits protein secretion. J Biol Chem. 2009; 284:4705–4712. [PubMed: 19074433]
44. Hinson ER, Cresswell P. The antiviral protein, viperin, localizes to lipid droplets via its N-terminal amphipathic alpha-helix. Proc Natl Acad Sci U S A. 2009; 106:20452–20457. [PubMed: 19920176]
45. Farese RV Jr, Walther TC. Lipid droplets finally get a little R-E-S-P-E-C-T. Cell. 2009; 139:855–860. [PubMed: 19945371]
46. Swann JB, Hayakawa Y, Zerafa N, Sheehan KC, Scott B, Schreiber RD, et al. Type I IFN contributes to NK cell homeostasis, activation, and antitumor function. J Immunol. 2007; 178:7540–7549. [PubMed: 17548588]
47. Trinchieri G. Type I interferon: friend or foe? J Exp Med. 2010; 207:2053–2063. [PubMed: 20837696]
48. Qian BZ, Pollard JW. Macrophage diversity enhances tumor progression and metastasis. Cell. 2010; 141:39–51. [PubMed: 20371344]

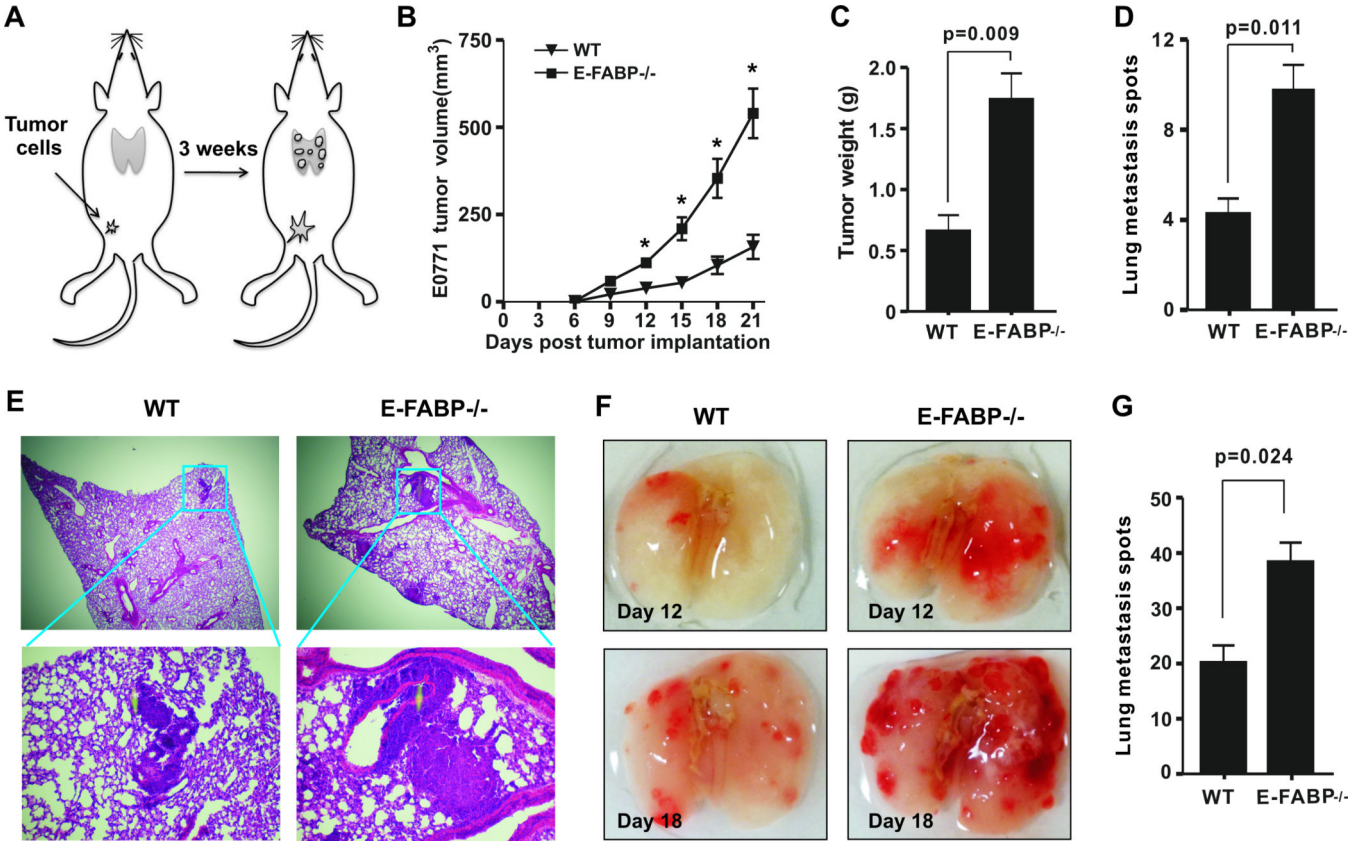

Figure 1. E-FABP protects mice from mammary tumor growth

A, schematic of the experimental procedure. B, E0771 cells (0.2×10^6) were orthotopically injected into the mammary pad of E-FABP$^{-/-}$ and WT mice (n=9/group). Tumor growth was measured at 3 day intervals. Weight of tumor mass (C), tumor metastasis spots (D) and H&E staining of lungs (E) were analyzed on day 24 after E0771 cell implantation in mice. Representative lung images (F) and tumor spots in lungs (G) on day 18 after tail vein injection of E0771 cells (0.2×10^6) in mice. Data represent mean ± SD (*, $p < 0.05$)

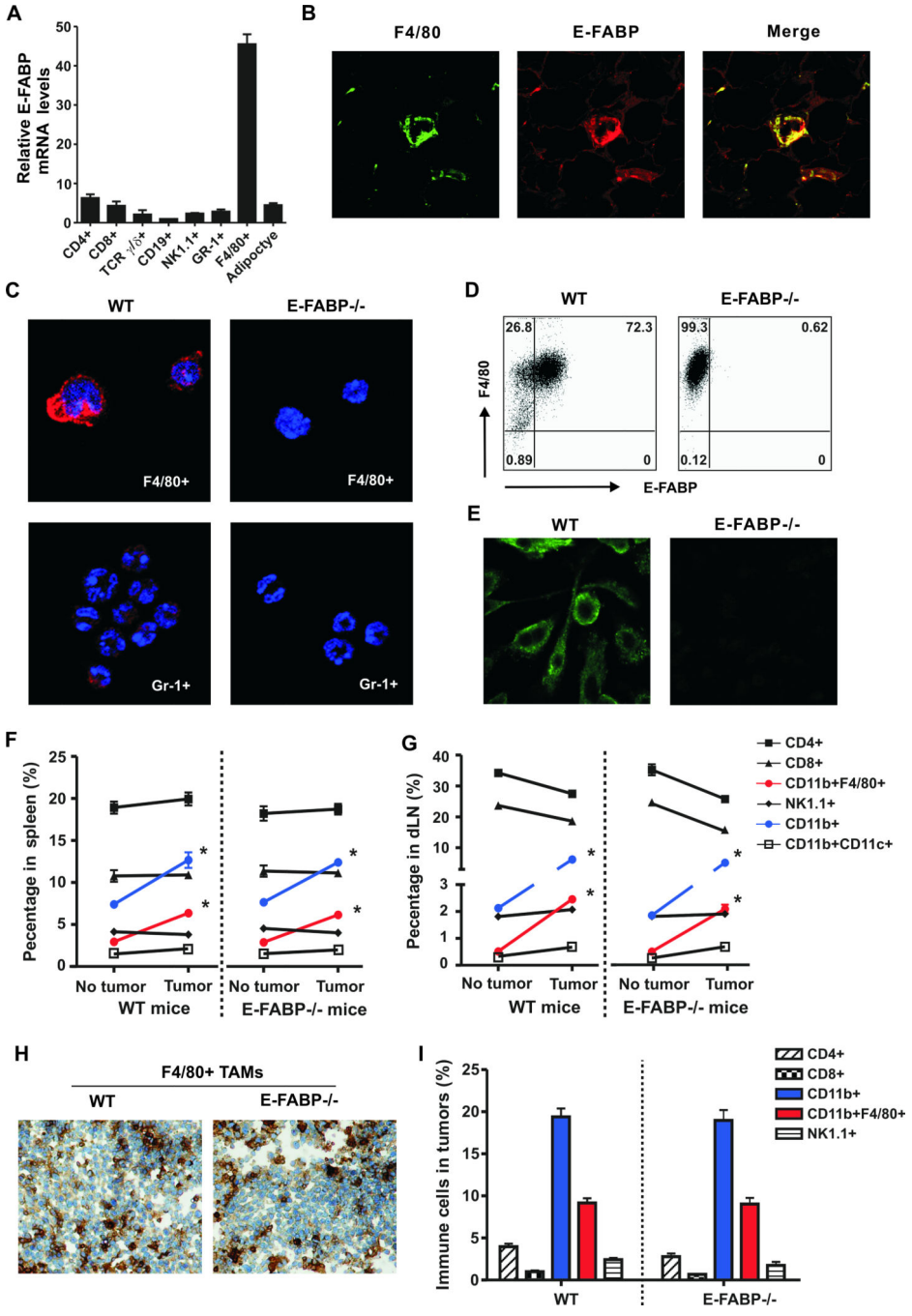

Figure 2. Analysis of E-FABP expression profile

A, real-time PCR analysis of E-FABP expression in splenic immune cells separated by a flow sorter. Adipocytes isolated from normal mammary fat pad were used as a control. B, analysis of F4/80^{+} macrophages (green) and E-FABP expression (red) in mammary fat tissues by confocal microscopy. C, analysis of E-FABP expression (red) in immune cells (nuclei,DAPI) separated from peripheral blood of mice. Analysis of E-FABP expression in bone marrow-derived macrophages by intracellular staining (D) and confocal microscopy (E). Phenotype analysis of immune cells in the spleen (F) and draining lymph nodes (dLN)

(G) of naïve and tumor-bearing mice (3 weeks post E0771 cell implantation) by flow cytometry (n=6/group). Analysis of $F4/80^+$ macrophages by immunohistochemistry staining (H) and immune cell populations by flow cytometry (I) in tumors 3 weeks after E0771 cell implantation. Data represent mean ± SD (*, $p < 0.05$).

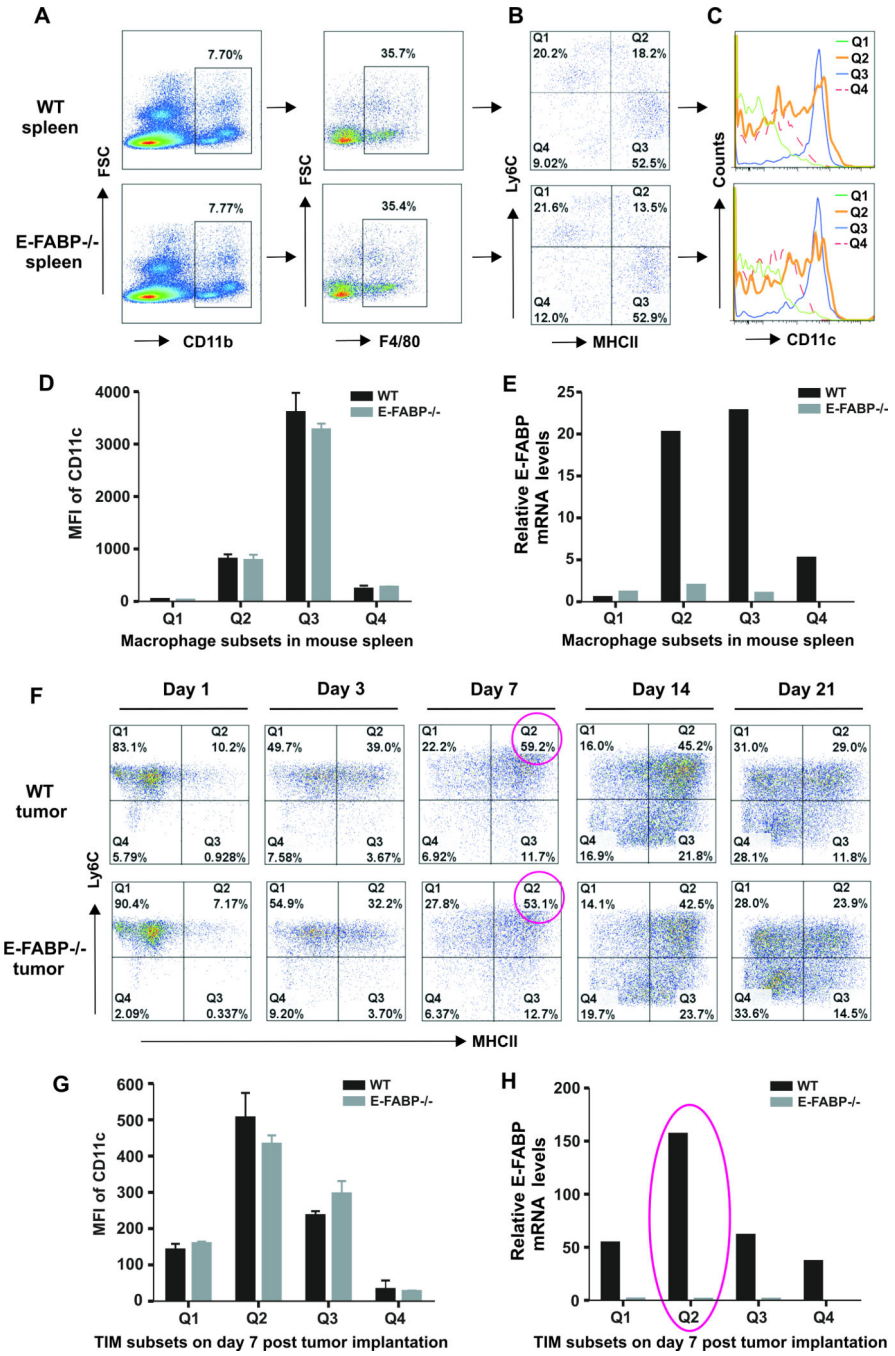

Figure 3. E-FABP is highly expressed in specific subsets of macrophages

A, identification of $CD11b^{+}F4/80^{+}$ macrophages from mouse spleen. B, distinct subsets of splenic macrophages by Ly6C and MHC-II staining. Analyses of CD11c expression by flow histogram (C) and mean fluorescent intensity (MFI) (D), and E-FABP expression by real-time PCR (E) in distinct macrophage subsets. F, flow cytometric analysis of dynamic changes of distinct subsets of TAMs in tumor stroma at indicated time points after E0771 cell implantation. Analysis of CD11c expression by MFI (G) and E-FABP expression by real-time PCR (H) in distinct subsets of TAMs on day 7 post E0771 cell implantation.

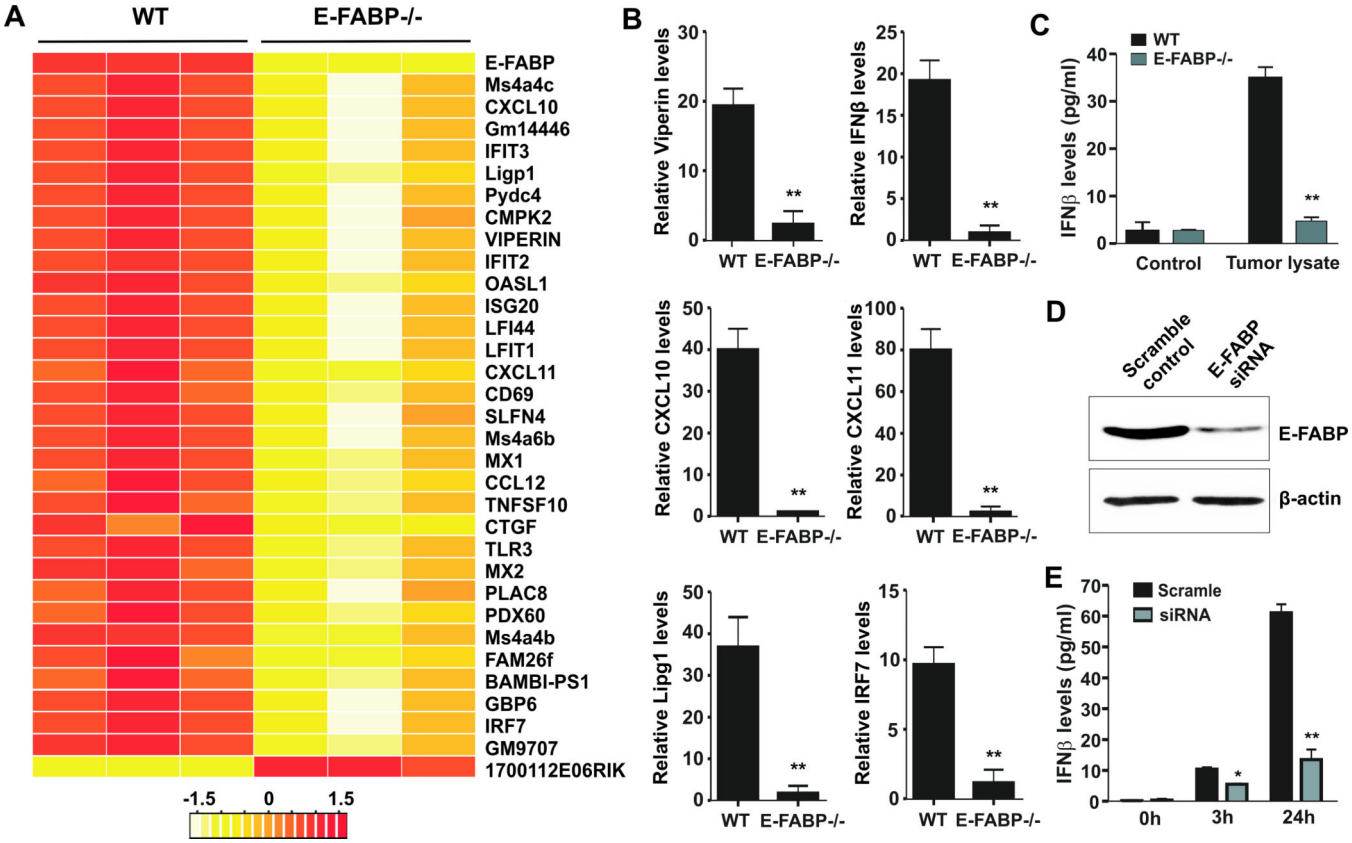

Figure 4. Microarray analysis of E-FABP-regulated genes in macrophages

A, a heat map of differentiated genes in E0771-stimulated GM-BMMs by Affymetrix microarray analysis. B, real-time PCR confirmation of interested E-FABP-regulated genes identified by microarray. C, IFNβ levels in the supernatants collected from GM-BMMs after stimulation with E0771 lysates for 3 hours by ELISA. D, analysis of E-FABP expression in macrophages transfected with E-FABP siRNA or scrambled oligos by western blotting. E, IFNβ levels in supernatants collected from macrophages as described in panel D in response to LPS at indicated time points. Data represent mean ± SD (*, $p < 0.05$, **, $p < 0.01$).

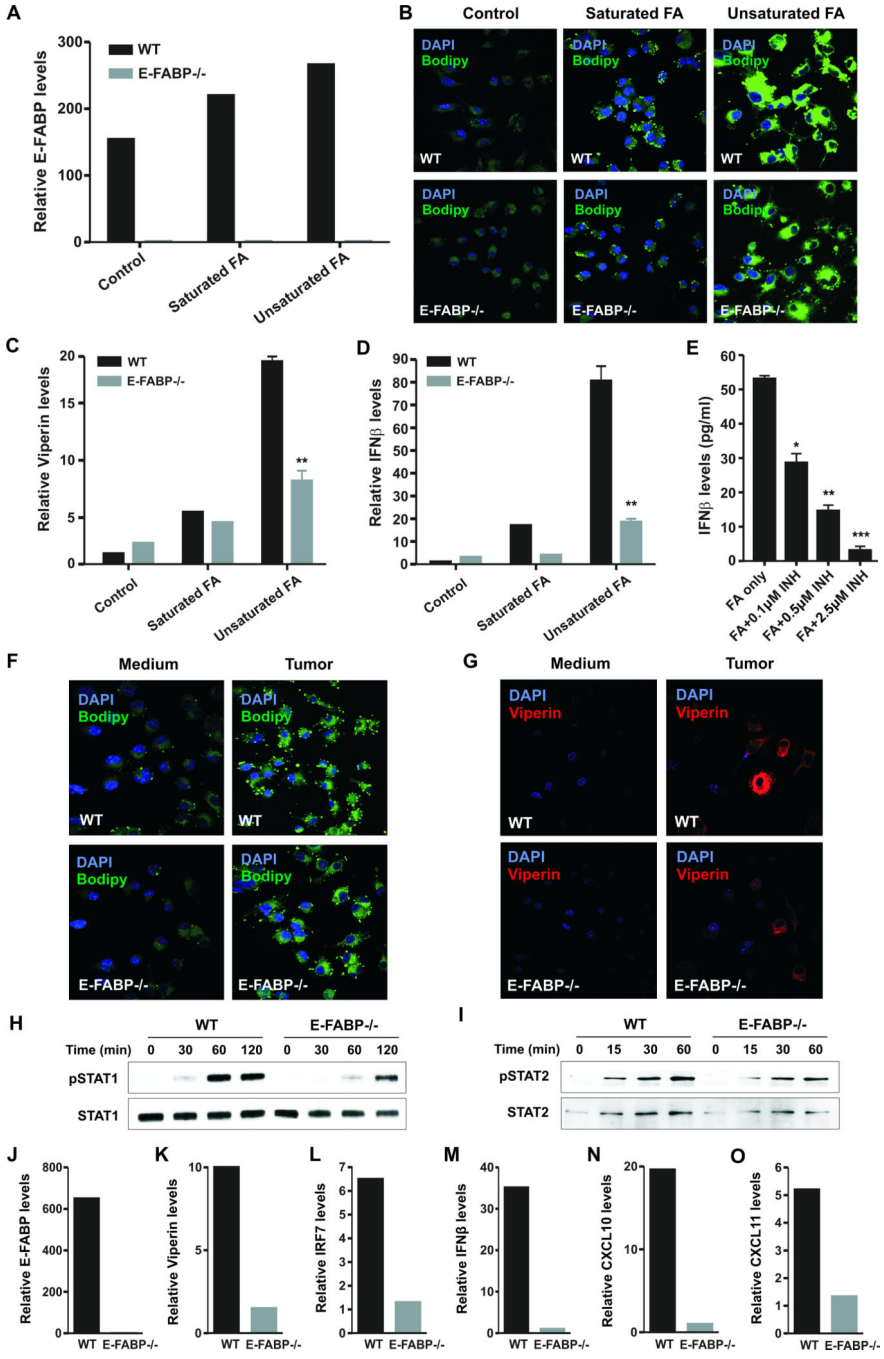

Figure 5. E-FABP promotes IFNβ responses by enhancing LD formation in macrophages

GM-BMMs were cultured with or without saturated FAs (stearic acid, 100μM) or unsaturated FAs (oleic/linoleic acid, 25μM) for 24 hr. E-FABP expression (A), LD formation (B), Viperin (C) and IFNβ (D) expression in these cells were measured by real-time PCR or confocal microscopy. E, analysis of IFNβ levels in supernatants of unsaturated FA-treated macrophages in the absence or presence of indicated LD inhibitor (Triacsin C) by ELISA. Analysis of LD formation (F) and Viperin expression (G) in GM-BMMs after coculture with or without E0771 tumor cells in a transwell for 18 hours by confocal

microscopy. Analysis of phosphorylation of STAT1 (H), STAT2 (I), and their total proteins in GM-BMMs after stimulation with 100U IFNβ for the indicated time periods. Expression of E-FABP (J), Viperin (K), IRF7 (L), IFNβ (M), CXCL10 (N), CXCL11 (O) in the Q2 subset of TAMs (separated from tumors on day 7 post E0771 cell implantation) was analyzed by real-time PCR. Data represent mean ± SD (*, $p < 0.05$, **, $p < 0.01$).

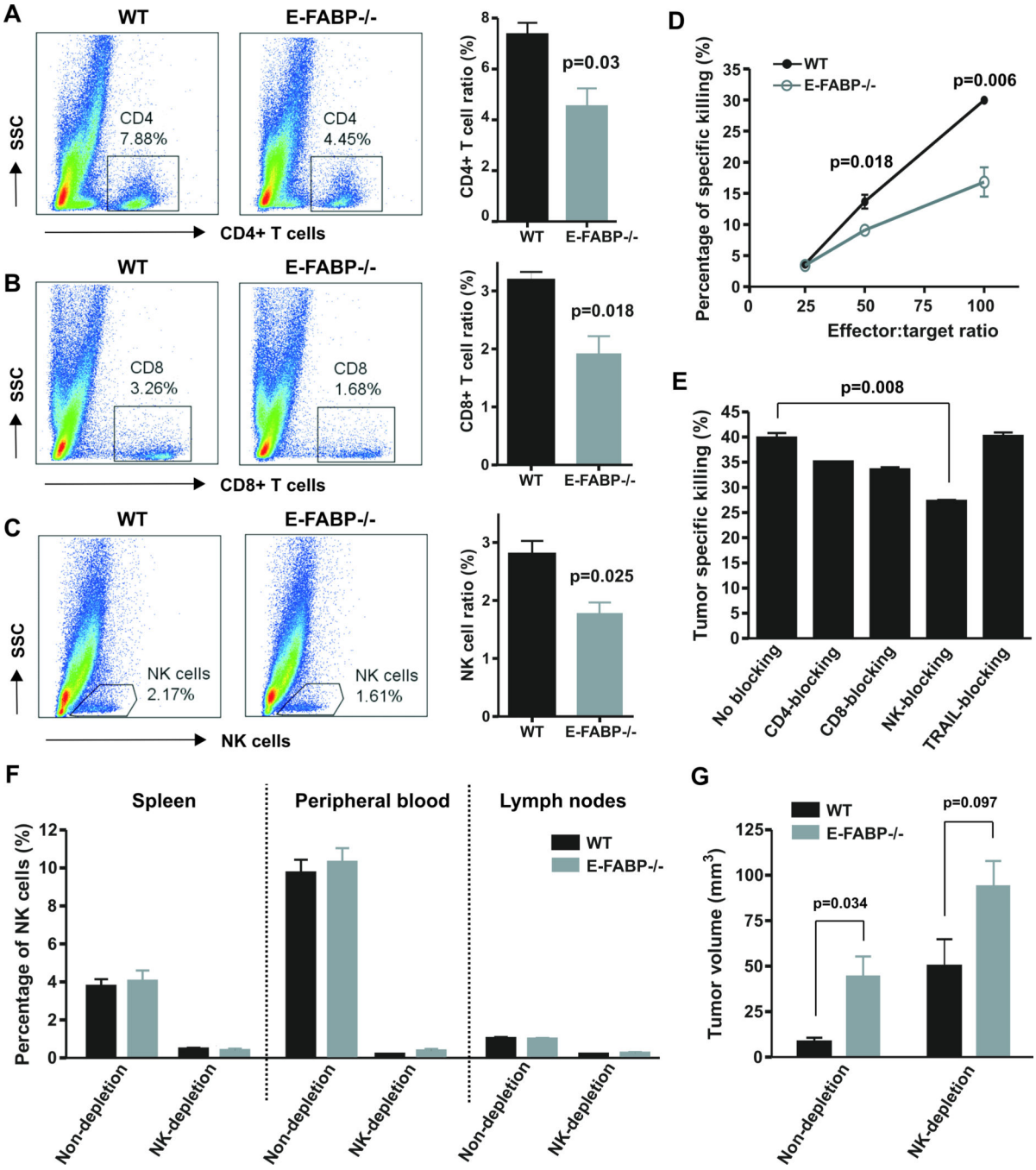

Figure 6. E-FABP enhances recruitment of tumoricidal effector cells

Analysis of infiltrated $CD4^+$ T cell (A), $CD8^+$ T cells (B) and NK cells (C) in tumors on day 7 post E0771 cell implantation in mice by flow staining. The percentage of each population was shown in the right panel. D, target cells (E0771) were labeled with CFSE and cocultured with effector cells (collected from dLNs of E0771-tumor bearing mice) at the indicated ratio. The percentage of specific tumor killing was analyzed by a flow cytometer. E, tumor specific killing assays as described in panel D (effect/target ratio:100) were performed in the absence or presence of respective blocking antibody to CD4, CD8, NK1.1

and TRIAL. F, Percentage of NK cells in spleen, peripheral blood and lymph nodes in mice with or without NK cell depletion. G, measurement of tumor size two weeks after E0771 cell implantation in WT and E-FABP$^{-/-}$ mice with or without NK cell depletion.

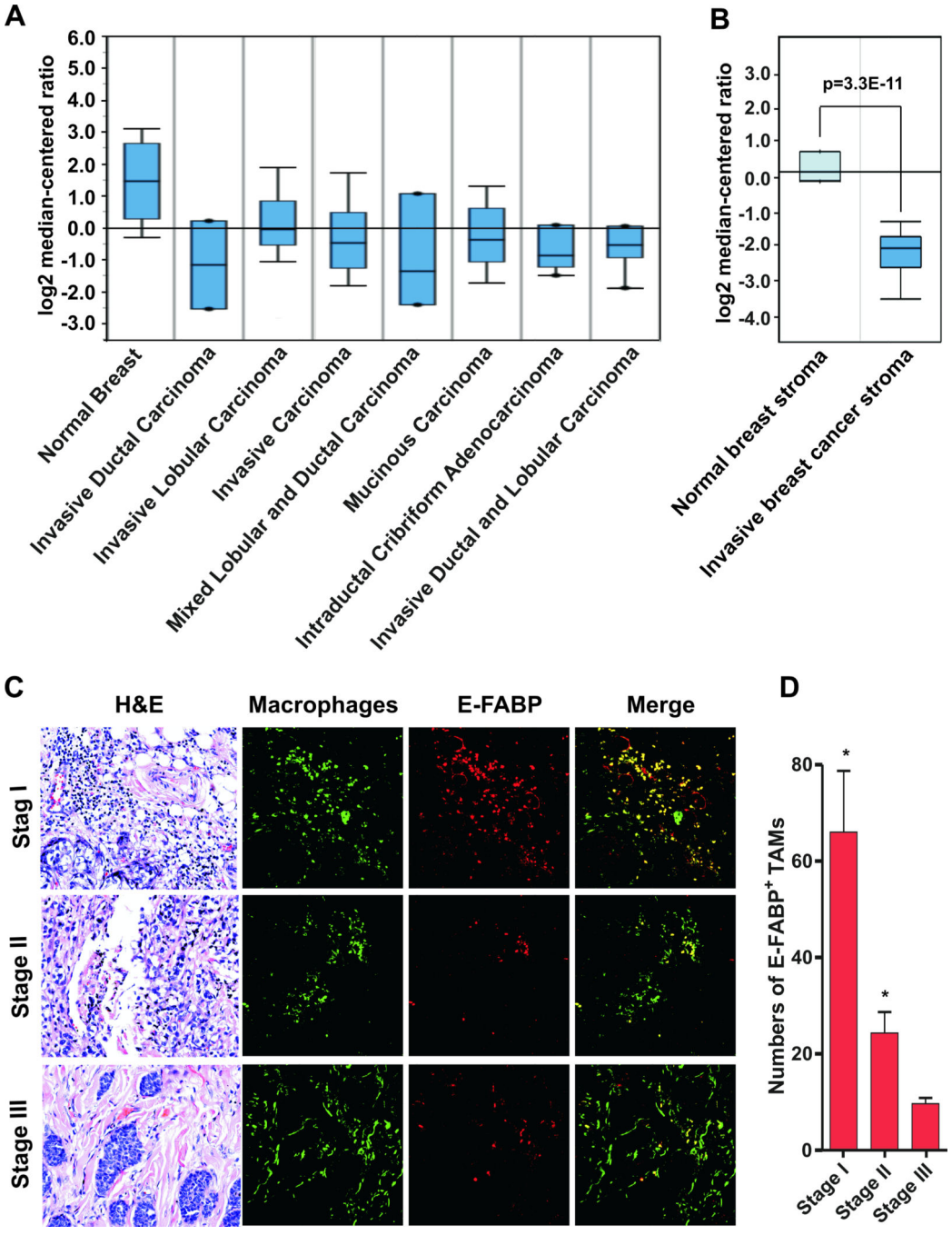

Figure 7. E-FABP expression in TAMs of human breast cancer

A, analysis of E-FABP expression in normal breast tissues and various types of malignant breast tissues from the publicly accessible microarray databases (www.oncomine.org/resouce). B, E-FABP expression in the stroma of normal and malignant breast tissues by analyzing GEO dataset GSE9014. C, co-staining of E-FABP expression (red) and TAMs (green) in different stages of invasive breast cancer tissues by confocal microscopy. H&E staining of the same section was shown on the left panel. D, numbers of E-FABP$^+$ TAMs

per high power fields (×400 magnification) were shown as mean ± SD. *p<0.05 as compared to stage III invasive breast cancers.